Trends in Biomaterials and Artificial Organs
sbaoi
journal homepage: www.biomaterials.org.in/tibao
ISSN (P) 0971-1198

Original Article

Modulation of Wound Healing Markers by Multicomponent Piezoelectric Nanofibrous Dressings: A Quantitative Immunohistochemical Study

Sobha Kota[1]*, Ratna Kumari Anantha[2]

[1]*RVR & JC College of Engineering (A) Campus, RVR & JCCE STP Foundation, Guntur 522019, Andhra Pradesh, India*
[2]*Department of Research, Sibar Institute of Dental Sciences, Guntur 522509, Andhra Pradesh, India*

Received: *23 May 2026*
Accepted: *13 July 2026*
Published online: *30 July 2026*

Keywords: *multicomponent dressings, excision wounds, immunohistochemistry, tissue biomarkers, wound healing*

The present investigation evaluated the therapeutic performance of multicomponent nanofibrous piezoelectric wound dressings using immunohistochemical analysis of major wound-healing biomarkers. Excisional wound tissues collected from Yorkshire pig models on day 34 after injury were examined for the expression of vascular endothelial growth factor (VEGF), alpha-smooth muscle actin (α-SMA), tumour necrosis factor-α (TNF-α), and transforming growth factor-β3 (TGF-β3). Quantitative assessment of stained tissue regions was carried out with Leica LAS imaging software to compare the biological responses among the treatment groups. Among the tested formulations, WD4 exhibited significantly higher TGF-β3 expression than the Standard Care group (Tukey HSD, $P < 0.05$), whereas the remaining comparisons were not statistically significant. WD4-treated wounds exhibited relatively lower TNF-α expression than WD2 and the Standard Care group; however, these differences were not statistically significant. One-way ANOVA demonstrated a significant difference in α-SMA expression among the groups ($P < 0.05$). Tukey HSD analysis further showed significantly higher α-SMA expression in the WD4 group than the standard care group, while the negative control also differed significantly from the standard care group. In addition, VEGF expression gradually increased in the treated groups, with WD4 exhibiting the highest VEGF expression among the treatment groups; however, the differences were not statistically significant. Overall, WD4 demonstrated favourable modulation of multiple wound-healing biomarkers, with statistically significant improvements observed for TGF-β3 and α-SMA relative to the standard care group, while TNF-α and VEGF showed non-significant directional trends. These results support the potential application of multicomponent nanofibrous piezoelectric dressings as advanced biomaterials for future clinical wound-care strategies.

Introduction

Inflammation, cell proliferation, angiogenesis, extracellular matrix (ECM) deposition, and tissue remodeling are all coordinated steps in the intricate biological process of wound healing, which eventually restores damaged tissue's structural and functional integrity. Each stage of repair is regulated by distinct cytokines, growth factors, and cellular interactions that can be effectively visualized through histochemical and immunohistochemical (IHC) techniques [1, 2]. Transforming growth factor-β (TGF-β), tumor necrosis factor-α (TNF-α), alpha-smooth muscle actin (α-SMA), and vascular endothelial growth factor (VEGF) are among the biomarkers commonly linked to wound repair, and their functions in inflammation, angiogenesis, fibrosis, and tissue remodeling are well known [3,4].

TGF-β plays an important role in fibroblast proliferation, extracellular matrix synthesis, and scar formation during tissue repair. The biological effects of this cytokine depend largely on its isoforms, where TGF-β1 and TGF-β2 are generally associated with fibrosis, while TGF-β3 has been linked to regenerative healing and reduced scar formation [5, 6]. TNF-α functions as an early inflammatory mediator released primarily by macrophages and keratinocytes. Although transient TNF-α activity supports immune cell recruitment and microbial defense, prolonged elevation may impair epithelialization and matrix remodeling [7,8]. VEGF is considered a major regulator of angiogenesis and vascular permeability, stimulating endothelial cell proliferation and neovascularization within granulation tissue [9,10]. In contrast, α-SMA

*Corresponding author: Dr. Sobha Kota
E-mail address: sobhakota2005@gmail.com

https://doi.org/10.65795/1c0bmp97

serves as a marker of activated myofibroblasts responsible for wound contraction and extracellular matrix remodeling under biochemical and mechanical stimulation [11,12]. Collectively, these markers provide a useful framework for assessing different phases of wound healing at the tissue level.

Although rodent models are commonly used during preliminary wound-healing investigations, large-animal models such as pigs and sheep provide greater translational relevance because their skin architecture, collagen organization, and healing characteristics closely resemble those of humans [13,14]. In particular, porcine skin demonstrates similarities to human skin with respect to epidermal turnover, dermal structure, and healing kinetics, making it highly suitable for evaluating biomaterials and regenerative therapies [15,16]. Ovine models are also valuable for studying large wounds and deeper dermal repair, especially in biomaterial and stem-cell-based applications [17,18]. Quantitative assessment of TGF-β, TNF-α, α-SMA, and VEGF expression in these models enables direct evaluation of inflammation, angiogenesis, fibroblast activation, and matrix remodeling during tissue repair, thereby strengthening the translational significance of preclinical studies [19, 20].

Despite substantial progress in the development of nanofibrous wound dressings, only limited studies have systematically correlated biomaterial-driven biointerface interactions with immunohistochemical markers associated with inflammation, angiogenesis, wound contraction, and regenerative remodeling in clinically relevant animal models. Addressing this gap is essential for improving biomaterial design strategies and enhancing the predictive value of translational wound-healing research.

Materials and Methods

Fabrication of wound dressings

The bioactive formulations of the wound dressings [21-23] designated as WD2 (CGCaP/PLL-H) and WD4 (CGCaP/PEO-H) consisted of deionized water (25 ml), glacial acetic acid (5 ml), chitosan (0.5 g), gelatin (0.5 g), and polyvinyl alcohol at a concentration of 2 g in WD2 and 1 g in WD4. Additionally, WD2 contained poly-L-lysine (750 μg), whereas WD4 was incorporated with polyethylene oxide (0.6 g). The core and shell nanofiber systems were composed of acetone (15 ml), acetone-extracted phytochemicals (8 ml), isopropanol (2.5 ml), IPA-extracted phytochemicals (5 ml), cellulose acetate (2 g), and keratin (0.25 ml in the shell layer). Taurine (0.02 g) was included in the core solution. Flow charts indicating the preparation of individual electrospinning solutions are provided in the supplementary material (figures S1 to S3).

The wound dressings were fabricated using a coaxial electrospinning approach. The base of the matrix consists of a cotton fabric pre-coated with copper oxide nanoparticles. Directly onto this modified fabric base, the core and shell solutions were electrospun via coaxial electrospinning using an electrospinning machine (Royal Enterprise, Chennai, India). After every layer of core-shell fibers, a layer of active solution-derived nanofibers was laid, and thus the scaffold is multilayered. Sobha et al. [24] described the specific chemical compositions of the core, shell, and active solutions used for electrospinning, together with the optimized processing parameters of voltage ranging from 15 to 25 kV, a flow rate of 4 to 6 ml/h, and a needle-to-collector distance of 20 cm.

Characterization of wound dressings

The morphology of the fabricated wound dressings (WD2 and WD4) was examined using field emission scanning electron microscopy (FESEM) to evaluate the fiber architecture and surface characteristics (AMETEK, Advanced Microanalysis Solutions). The average fiber diameter was determined from representative micrographs using Image J software by measuring randomly selected fibers. The piezoelectric behaviour of the electrospun membranes was assessed using piezoresponse force microscopy (PFM) (MFP-3D-BIOV15, Asylum Research, Santa Barbara, CA, USA, and Igor Pro V6), where amplitude and phase responses were recorded to investigate their local electromechanical properties. The zeta potential of the dressing in solution was estimated using a Horiba SZ-100.

The fabricated multicomponent nanofibrous piezoelectric wound dressings were evaluated in three experimental animals identified as P1, P2, and P3, and every animal received eight wounds with all treatment conditions (negative control, standard care, WD2, and WD4) according to a balanced wound-allocation matrix [24]. The in vivo investigation focused on comparing these optimized dressings with clinically relevant controls, namely standard care (Iodine-Povidone solution) and untreated wounds (negative control). As the study design approved by the IEAC allowed experiments with three pigs, the number of controls was chosen optimally in compliance with the recommendations of the Committee for the Control and Supervision of Experiments on Animals (CCSEA) (Certification Number: 1312/PO/RcBiBt-S/RcBiBt-L/09/CPCSEA).

The animals were put to death by overdosing on thiopentone injection on day 34 following wound induction. Samples of the wound tissue were taken and stored in 10% neutral buffered formalin. A veterinary pathologist conducted a holistic pathological examination of every animal to find any significant internal or external abnormalities. As described in the supplementary material, wound tissues were processed for immunohistochemical analysis using tissue sections measuring approximately 2–3 μm in thickness. The research pathologist then looked at the produced slides using a light microscope. Quantitative analysis of the percent-stained area for TGF-β3, TNF-α, α-SMA, and VEGF was carried out using Leica LAS imaging software.

Results

Characterization of wound dressings

Characterization of WD2 and WD4 demonstrated that the fabricated electrospun dressings possessed the structural and functional properties required for wound healing applications. FESEM images revealed a uniform, bead-free fibrous network with an interconnected porous architecture, while fiber diameter measurements confirmed consistent fiber formation. PFM analysis verified the electromechanical activity of the membranes through characteristic amplitude and phase responses, indicating that the electrospun fibers retained their piezoelectric functionality. Together, these findings indicate that WD2 and WD4 combine favourable morphology and piezoelectric responsiveness, supporting their potential as multifunctional wound dressing materials.

The physicochemical characterization of WD2 and WD4 confirmed the successful fabrication of electrospun wound dressings with properties favourable for wound healing applications. FESEM analysis revealed uniform, bead-free nanofibrous architecture with interconnected pores, while fiber diameter measurements were 135.7 ± 34.7 nm for WD2 (figure S4) and 151.5 ± 46.7nm for WD4 (figure S5). Piezoresponse force microscopy further confirmed the electromechanical behaviour of the dressings, with piezoelectric coefficients of 24.03 pm/V for WD2 and 28.15 pm/V for WD4 (figure S6), demonstrating the retention of piezoelectric functionality following electrospinning [24]. These findings demonstrate that WD2 and WD4 possess the structural integrity and

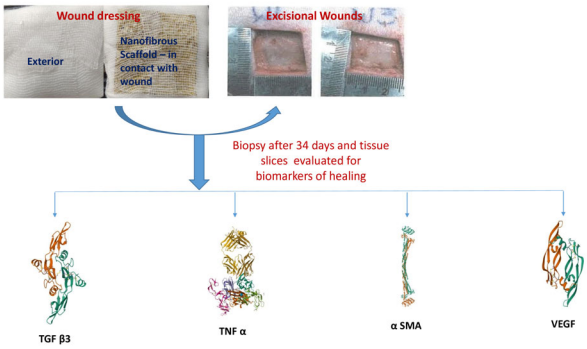

Figure 1: Multicomponent nanofibrous dressings used for histochemical evaluation of four key biomarkers in wound healing

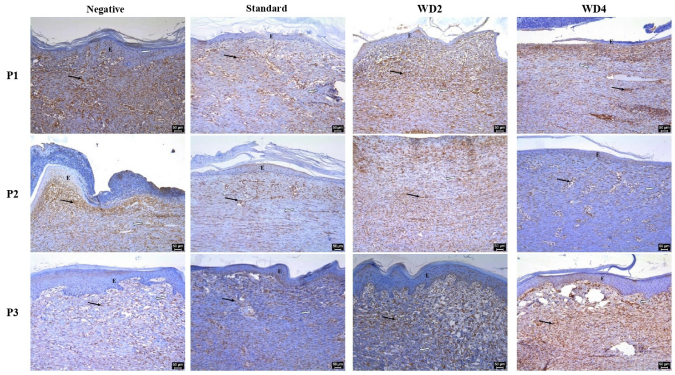

Figure 2: TGF-β3 expression in the tissue sections of the three experimental animals after 34 days (10x and 50µm scale)

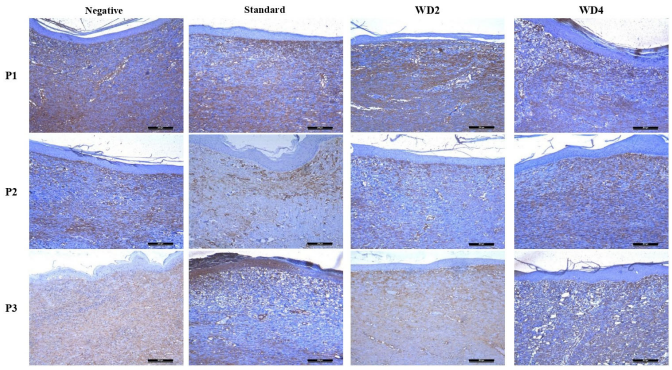

Figure 3: TNF-α expression in the tissue sections of the three experimental animals after 34 days (10× and 200µm scal

piezoelectric properties required for wound dressing applications. Zeta potential analysis showed high positive charges for both formulations (WD2: +57.7 mV; WD4: +94.6 mV), suggesting excellent colloidal stability and enhanced potential for interaction with cells (figure S7).

The four reported biomarkers (figure 1) were selected to represent key biointerface-responsive pathways associated with regenerative remodeling (TGF-β3), inflammation (TNF-α), angiogenesis (VEGF), and myofibroblast-mediated contraction (α-SMA).

Transforming growth factor β3

Immunohistochemical examination demonstrated detectable TGF-β3 expression in all experimental groups, confirming its involvement during the wound-healing process (figure 2). The lowest mean percent-stained area was recorded in the Negative Control group (12.85), followed closely by the Standard Care group (13.14). In comparison, wounds treated with WD2 and WD4 exhibited higher TGF-β3 expression, with mean values of 15.74 and 17.17, respectively (table 1). WD2- and WD4-treated wounds exhibited higher TGF-β3 expression than the control groups. Although the overall ANOVA did not demonstrate a significant difference among all groups ($F = 2.25$, $P \geq 0.09$), Tukey HSD analysis identified a significant difference between the Standard Care and WD4 groups ($P = 0.0368$) (table 2).

Table 1: Percent-stained area TGFâ3, TNF-α, α-SMA and VEGF of wounds treated with Negative, Standard, WD2 and WD4

Treatment	Animal	Wound	Percent-stained area			
			TGFβ3	TNF-α	α-SMA	VEGF
Negative	P1	W7	8.78 ± 0.42	7.63 ± 0.71	15.69 ± 3.1	2.86 ± 0.76
		W8	25.68 ± 1.5	8.95 ± 1.44	17.12 ± 4.54	3.57 ± 1.93
	P2	W1	10.5 ± 0.1	7.92 ± 0.7	13.27 ± 5.4	4.18 ± 0.66
		W2	10.21 ± 0.56	3.07 ± 0.46	10.24 ± 0.96	1.64 ± 0.4
	P3	W3	11.28 ± 0.06	9.3 ± 7.34	16.44 ± 3.28	9.55 ± 2.47
		W4	10.65 ± 0.13	6.68 ± 0.29	8.25 ± 2.14	2.82 ± 2.78
	Average ± SD		**12.85 ± 0.54**	**7.26 ± 2.73**	**13.5 ± 1.6**	**4.1 ± 1.02**
Standard	P1	W1	14.36 ± 0.71	6.07 ± 0.11	6.65 ± 3.72	10.18 ± 0.38
		W2	11.77 ± 0.1	13.17 ± 7.9	13.7 ± 6.4	3.22 ± 1.41
	P2	W3	16.24 ± 0.82	5.83 ± 0.7	4.95 ± 0.19	3.47 ± 0.38
		W4	9.09 ± 0.00	6.23 ± 1.16	9.03 ± 5.17	3.53 ± 0.55
	P3	W5	12.5 ± 1.65	16.03 ± 1.98	9.48 ± 0.4	1.77 ± 0.26
		W6	14.92 ± 1.12	23.48 ± 1.02	12.68 ± 0.95	5.49 ± 2.38
	Average ± SD		**13.14 ± 0.62**	**11.8 ± 2.88**	**9.41 ± 2.66**	**4.61 ± 0.84**
WD2	P1	W3	23.84 ± 1.47	9.75 ± 0.96	10.6 ± 5.03	4.55 ± 9.95
		W4	14.78 ± 0.19	19.82 ± 1.14	16.23 ± 1.32	8.66 ± 4.99
	P2	W5	13.45 ± 0.0	7.52 ± 1.54	8.76 ± 0.95	5.27 ± 3.67
		W6	14.75 ± 3.88	2.72 ± 0.00	14.8 ± 4.6	4.64 ± 1.92
	P3	W7	14.89 ± 0.04	13.14 ± 8.84	11.06 ± 5.83	3.44 ± 0.97
		W8	12.72 ± 0.03	13.99 ± 3.72	12.17 ± 2.46	1.9 ± 1.01
	Average ± SD		**15.74 ± 1.55**	**11.16 ± 3.25**	**12.27 ± 2.06**	**4.74 ± 2.11**
WD4	P1	W5	22.03 ± 0.1	5.36 ± 0.14	11.74 ± 2.58	4.37 ± 1.74
		W6	21.73 ± 0.63	20.26 ± 1.43	15.73 ± 1.75	7.61 ± 6.04
	P2	W7	13.78 ± 0.51	3.85 ± 1.02	15.26 ± 3.01	3.84 ± 3.61
		W8	9.77 ± 1.79	6.6 ± 0.11	13.11 ± 3.53	6.29 ± 1.15
	P3	W1	23.65 ± 0.03	7.34 ± 0.39	13.72 ± 1.54	11.2 ± 1.2
		W2	12.05 ± 0.02	15.05 ± 0.2	10.99 ± 1.53	2.19 ± 0.47
	Average ± SD		**17.17 ± 0.68**	**9.74 ± 0.55**	**13.43 ± 0.84**	**5.92 ± 2.09**

Table 2: One-way ANOVA and Tukey HSD pairwise comparison of TGF-β3, TNF-α, α-SMA, and VEGF expression among the Negative Control, Standard Care, WD2, and WD4 groups

Biomarker	One-way ANOVA	Negative vs. Standard	Negative vs. WD2	Negative vs. WD4	Standard vs. WD2	Standard vs. WD4	WD2 vs. WD4
TGFβ3	F value	0.02372	1.8778	3.2104	3.5119	4.942	0.4934
	P value	0.879	0.1844	0.08694	0.07427	0.0368*	0.4898
	Tukey HSD	NSD	NSD	NSD	NSD	SD	NSD
TNF-α	F value	3.9494	3.6344	1.5392	0.0535	0.5588	0.3059
	P value	0.05948	0.06974	0.2278	0.8192	0.4626	0.5858
	Tukey HSD	NSD	NSD	NSD	NSD	NSD	NSD
α-SMA	F value	5.4908	0.5358	0.002567	2.9734	7.9496	0.7407
	P value	0.02856*	0.4719	0.9601	0.09867	0.009983*	0.3987
	Tukey HSD	SD	NSD	NSD	NSD	SD	NSD
VEGF	F value	0.173	0.2369	1.6967	0.01059	0.8863	0.6301
	P value	0.6815	0.6313	0.2062	0.919	0.3567	0.4358
	Tukey HSD	NSD	NSD	NSD	NSD	NSD	NSD

Note: SD - Significant difference ($p<0.05$); NSD - No significant difference ($p>0.05$)

Tumour necrosis factor (TNF-α)

Noticeable variation in TNF-α expression was observed among the experimental groups (figure 3). The Negative Control group demonstrated the lowest mean percent-stained area (7.26), whereas the Standard Care group showed a marked increase (11.8). A comparable level of TNF-α expression was detected in WD2-treated wounds (11.16), while WD4-treated wounds displayed relatively lower expression (9.74) compared to WD2 and Standard Care groups (table 1). WD4-treated wounds exhibited relatively lower TNF-α expression than WD2 and the Standard Care group. However, neither the overall ANOVA nor Tukey HSD analysis demonstrated statistically significant differences among the treatment groups (table 2). Therefore, these findings are interpreted as non-significant biological trends. These findings suggest that WD2 maintained an active inflammatory response required during the healing phase, whereas the moderated TNF-α expression observed in WD4 may indicate progression toward inflammation resolution and transition into the proliferative stage of repair.

Alpha-smooth muscle actin (α-SMA)

α-SMA expression, which reflects myofibroblast activation and wound contraction, was prominently detected in the negative control (13.5) and WD4 (13.43) groups, both demonstrating comparable mean percent-stained areas (table 1, figure 4). WD2-treated wounds showed moderately elevated α-SMA expression (12.27), while the Standard Care group exhibited the lowest expression level (9.41). One-way ANOVA demonstrated significant differences in α-SMA expression among the experimental groups ($F = 3.02$, $P < 0.05$). Tukey HSD analysis revealed significantly higher α-SMA expression in WD4 compared with the Standard Care group ($P = 0.00998$). A significant difference was also observed between the negative control and Standard Care groups ($P = 0.0286$), whereas the remaining pairwise comparisons were not statistically significant (table 2).

Vascular endothelial growth factor (VEGF)

VEGF amount remained comparatively low across all experimental groups; however, treated wounds showed a gradual increase in expression levels (figure 5). The negative control group recorded the lowest mean percent-stained area (4.11), followed by the Standard Care group (4.61). WD2-treated wounds demonstrated a slight increase in VEGF expression (4.74), whereas WD4-treated wounds exhibited the highest mean expression (5.92) (table 1). However, neither one-way ANOVA nor Tukey HSD analysis demonstrated statistically significant differences among the groups (table 2). Elevated VEGF expression in WD4-treated wounds suggests enhanced angiogenic activity, which is important for neovascularization, oxygen supply, and granulation tissue development during wound healing.

Discussion

The coordinated modulation of TGF-β3, TNF-α, α-SMA, and VEGF observed in this study reflects a well-regulated wound-healing response in the treated groups. WD4 demonstrated significantly greater TGF-β3 expression than the Standard Care group, suggesting improved regen-

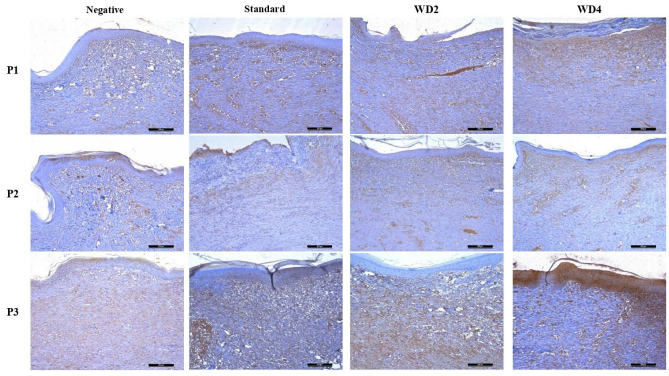

Figure 4: α-SMA expression in the tissue sections of the three experimental animals after 34 days (10× and 200μm scale)

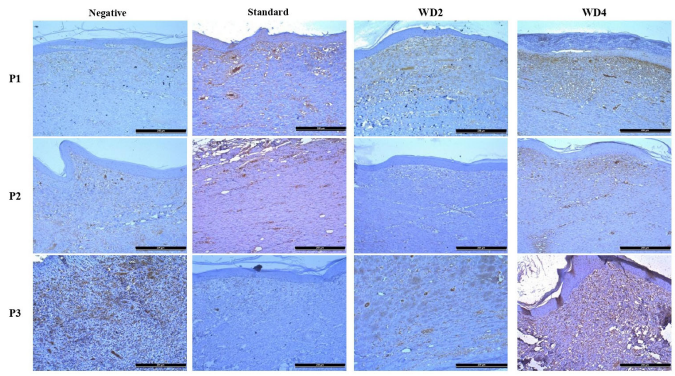

Figure 5: VEGF expression in the tissue sections of the three experimental animals after 34 days (10× and 200μm scale)

erative remodeling. This can be attributed to better tissue organization and less scar formation, according to earlier research, especially in translational large-animal wound models [5,17,18,25,26]. Although the remaining pairwise comparisons were not statistically significant, the overall expression pattern supports the regenerative potential of the developed dressing. An essential inflammatory cytokine in the initial phases of wound healing is TNF-α. While transient TNF-α activity is necessary for immune cell recruitment and defense against infection, prolonged elevation may impair tissue remodeling and delayed healing [7,8,27]. In the present investigation, WD4 exhibited relatively lower TNF-a expression than WD2 and the Standard Care group. However, these differences were statistically insignificant.

Myofibroblasts play an essential role in extracellular matrix remodeling and biomechanical stabilization during tissue repair [11,12,18]. The observed increase in α-SMA expression therefore suggests that the developed nanofibrous piezoelectric dressings positively influenced tissue remodeling and contractile healing responses. During wound healing, angiogenesis and neovascularization are primarily regulated by VEGF. Improved vascular development and the repairing tissue's oxygen supply are suggested by the slow rise in VEGF expression seen in the treated groups, especially in WD4. One-way ANOVA together with Tukey HSD analysis demonstrated significantly higher α-SMA expression in WD4 than in the Standard Care group, supporting enhanced myofibroblast activity and tissue remodeling induced by the developed dressing.

VEGF is a principal regulator of angiogenesis and neovascularization with improved oxygen supply within the healing tissue [9,10,16,29], assumed to be induced by the applied dressing. Balanced angiogenic signaling is critical for maintaining granulation tissue formation without promoting excessive or disorganized vessel growth [8]. Although WD4 exhibited the highest VEGF expression among the treatment groups, neither the overall ANOVA nor Tukey HSD analysis demonstrated statistically significant differences. These findings therefore suggest a favourable angiogenic trend that requires confirmation in larger studies.

Collectively, the findings demonstrate that multicomponent nanofibrous piezoelectric wound dressings can effectively regulate inflammatory, regenerative, angiogenic, and contractile pathways involved in tissue repair. Among the evaluated formulations, WD4 consistently exhibited the most balanced biological response, supporting its potential application in advanced wound-healing strategies and translational biomaterial research.

There are some noted limitations to this study. Only at the terminal trial endpoint (day 34), which was chosen to evaluate tissue remodeling and total wound recovery after therapy, was immunohistochemical assessment carried out. As a result, it was impossible to assess the temporal expression patterns of biomarkers linked to the proliferative and inflammatory stages of healing, especially TNF-α and VEGF. A more thorough knowledge of the dynamic biological reactions generated by the created wound dressings would be possible with future research that included numerous sampling time points (e.g., days 3,7,14, and 34).

This study's inability to measure the in vivo electrical output produced by the piezoelectric dressings is another limitation. The suggested process is predicated on the idea that the animals' typical physiological movements and the resulting skin deformation during regular walking may have supplied enough mechanical stimulation to trigger the piezoelectric fibers. Nevertheless, there was no direct measurement of the electrical impulses produced in the wound environment. Future studies that combine biological results with in vivo electrical data might shed further light on the molecular role of piezoelectric stimulation in wound healing.

Conclusion

The present study demonstrates that multicomponent nanofibrous piezoelectric wound dressings can effectively regulate molecular pathways associated with wound healing. Significant improvements in TGF-β3 and α-SMA expression relative to the standard care group, together with favourable but non-significant trends in TNF-α and VEGF expression, suggest that WD4 promotes multiple aspects of wound repair, including regenerative remodeling, wound contraction, inflammation resolution, and angiogenesis. Among the evaluated formulations, WD4 consistently exhibited the most balanced wound-healing response characterized by moderated inflammatory activity and enhanced regenerative signaling. Overall, these findings support the translational relevance of immunohistochemical biomarker assessment for evaluating advanced biomaterial-based wound dressings and their potential future clinical application.

Acknowledgements

The authors express their sincere gratitude to RVR & JCCE STP Foundation for providing biomedical laboratory support and encouragement. The first author expresses sincere gratitude for the sanction of Ignition Grant under DST NIDHI iTBI scheme of RVR & JCCE STP Foundation, RVR & JC College of Engineering (A) Campus, Guntur, AP, India. The study was conducted at Palamuru Biosciences Pvt. Ltd. in Hyderabad, Telangana, India, and the experiments were done in compliance with the protocols' approvals.

Supplementary Material: Supplementary material is available online for download.

References

1. Eming SA, Martin P, Tomic-Canic M, Wound repair and regeneration: mechanisms, signaling, and translation, Sci. Transl. Med., 6, 265sr6 (2014).
2. Gurtner GC, Werner S, Barrandon Y, Longaker MT, Wound repair and regeneration, Nature, 453, 314–321 (2008).
3. Werner S, Grose R, Regulation of wound healing by growth factors and cytokines, Physiol. Rev., 83, 835–870 (2003).
4. Barrientos S, Stojadinovic O, Golinko MS, Brem H, Tomic-Canic M, Growth factors and cytokines in wound healing, Wound Repair Regen., 16, 585–601 (2008).
5. Shah M, Foreman DM, Ferguson MW, Neutralisation of TGF-â1 and TGF-â2 or exogenous addition of TGF-â3 to cutaneous rat wounds reduces scarring, J. Cell Sci., 108, 985–1002 (1995).
6. Penn JW, Grobbelaar AO, Rolfe KJ, The role of the TGF-â family in wound healing, burns and scarring: a review, Int. J. Burns Trauma, 2, 18–28 (2012).
7. Gallucci RM, Sloan DK, Heck JM, Murray AR, O'Dell SJ, Interleukin-6 indirectly induces keratinocyte migration, J. Invest. Dermatol., 122, 764–772 (2004).
8. Eming SA, Wynn TA, Martin P, Inflammation and metabolism in tissue repair and regeneration, Science, 356, 1026–1030 (2017).
9. Ferrara N, Vascular endothelial growth factor: basic science and clinical progress, Endocr. Rev., 25, 581–611 (2004).
10. Tonnesen MG, Feng X, Clark RAF, Angiogenesis in wound healing, J. Investig. Dermatol. Symp. Proc., 5, 40–46 (2000).
11. Darby IA, Laverdet B, Bonté F, Desmoulière A, Fibroblasts and myofibroblasts in wound healing, Clin. Cosmet. Investig. Dermatol., 7, 301–311 (2014).
12. Hinz B, Myofibroblasts, Exp. Eye Res., 142, 56–70 (2016).
13. Sullivan TP, Eaglstein WH, Davis SC, Mertz P, The pig as a model for human wound healing, Wound Repair Regen., 9, 66–76 (2001).
14. Seaton M, Hocking A, Gibran NS, Porcine models of cutaneous wound healing, ILAR J., 56, 127–138 (2015).
15. Wang JF, Olson ME, Reno CR, Wright JB, Hart DA, The pig as a model for excisional skin wound healing, Comp. Med., 51, 341–348 (2001).
16. Kuo TY, Huang CC, Shieh SJ, Wang YB, Lin MJ, Wu MC, Huang LLH, Skin wound healing assessment via an optimized wound array model in miniature pigs, Sci. Rep., 12, 445 (2022).
17. Banstola A, Reynolds JNJ, The sheep as a large animal model for the investigation and treatment of human disorders, Biology (Basel), 11, 1251 (2022).
18. Martinello T, Gomiero C, Perazzi A, Iacopetti I, Gemignani F, DeBenedictis GM, Ferro S, Zuin M, Martines E, Brun P, Maccatrozzo L, Chiers K, Spaas JH, Patruno M, Allogeneic mesenchymal stem cells improve the wound healing process of sheep skin, BMC Vet. Res., 14, 202 (2018).
19. Ribitsch I, Baptista PM, Lange-Consiglio A, Melotti L, Patruno M, Jenner F, Schnabl-Feichter E, Dutton LC, Connolly DJ, Van Steenbeek FG, Dudhia J, Penning LC, Large animal models in regenerative medicine and tissue engineering, Front. Bioeng. Biotechnol., 8, 972 (2020).
20. Bernardelli de Mattos I, Tuca AC, Kukla F, Lemarchand T, Markovic D, Kamolz LP, Funk M, A highly standardized pre-clinical porcine wound healing model, Biomedicines, 12, 1697 (2024).
21. Kota S, Dumpala P, Sajja R, Anantha R, Phytoconstituents of Chromolaena odorata leaf extract for synthesis of CuO/Cu nanoparticles, Trends Phytochem. Res., 7, 186–206 (2023).
22. Kota S, Dumpala P, Sajja R, Anantha R, Heteroatom-doped carbon dots from medicinal plants as novel biomaterials, Sci. Rep., 14, 13160 (2024).
23. Kota S, Dumpala P, Sajja R, Anantha R, Functional characteristics of copper/copper oxide nanoparticles synthesized with plant extracts, Sci. Rep., 14, 30857 (2024).
24. Kota S, Anantha R, Sajja R, Dumpala P, Multicomponent nanofibrous electrospun dressings in a porcine model, 3 Biotech, 15, 335 (2025).
25. Le M, Naridze R, Morrison J, Biggs LC, Rhea L, Schutte BC, Kaartinen V, Dunnwald M,

Transforming growth factor beta 3 is required for excisional wound repair in vivo, PLoS One, 7, e48040 (2012).
26. Pastar I, Stojadinovic O, Yin NC, Ramirez H, Nusbaum AG, Sawaya A, Patel SB, Khalid L, Isseroff RR, Tomic-Canic M, Epithelialization in wound healing: a Comprehensive review, Adv. Wound Care, 3, 445–464 (2014).
27. Mohiti-Asli M, Risselada M, Jacob M, Pourdeyhimi B, Loboa EG, Creation and evaluation of a new porcine model for surgical site infection, Tissue Eng. Part C Methods, 23, 795–803 (2017).
28. Tuca AC, Bernardelli de Mattos I, Funk M, Markovic D, Winter R, Lemarchand T, Kniepeiss D, Spendel S, Hartmann B, Ottoman C, Kamolz LP, A standardized porcine model for partial-thickness wound healing, Int. J. Mol. Sci., 25, 7658 (2024).
29. Werner S, Grose R, Regulation of wound healing by growth factors and cytokines, Physiol. Rev., 83, 835–870 (2003).